文章编号:1007-9629(2025)04-0299-08

UHPC-NC刻槽界面剪切性能及抗剪强度计算方法

田　静[1,2]，　江星宏[3]，　杨新安[1,2,*]，　马明杰[1,2]，　李路恒[1,2]

(1.同济大学 道路与交通工程教育部重点实验室,上海 201804; 2.同济大学 交通学院,上海 201804; 3.招商局重庆交通科研设计院有限公司, 重庆 400067)

摘要:考虑普通混凝土(NC)强度等级、刻槽密度2个因素,通过斜剪试验和双面直剪试验,分析了超高性能混凝土-普通混凝土(UHPC-NC)刻槽界面在压剪和纯剪应力状态下的剪切性能,并基于试验结果给出了UHPC-NC刻槽界面抗剪强度计算公式以及此类界面斜剪试件的界面倾角范围.结果表明:界面倾角30°斜剪试件表现为NC压溃破坏或界面剪切+NC压溃组合破坏,界面倾角60°斜剪试件和直剪试件均表现为界面剪切破坏;试件强度与NC强度成正比,随着刻槽密度的增大,界面倾角30°斜剪试件的强度基本不变,界面倾角60°斜剪试件和直剪试件的强度逐渐增大;UHPC-NC刻槽界面的抗剪内摩擦角取决于NC强度等级.

关键词:UHPC-NC刻槽界面;界面抗剪强度;斜剪试验;双面直剪试验;刻槽密度

中图分类号:TU528.31　　**文献标志码**:A　　**doi**:10.3969/j.issn.1007-9629.2025.04.002

Shear Properties and Shear Strength Calculation Method of UHPC-NC Grooved Interface

TIAN Jing[1,2], *JIANG Xinghong*[3], *YANG Xinan*[1,2,*], *MA Mingjie*[1,2], *LI Luheng*[1,2]

(1. The Key Laboratory of Road and Traffic Engineering, Ministry of Education, Tongji University, Shanghai 201804, China; 2. College of Transportation Engineering, Tongji University, Shanghai 201804, China; 3. China Merchants Chongqing Communications Technology Research & Design Institute Co., Ltd., Chongqing 400067, China)

Abstract: Considering the two factors of normal concrete (NC) strength and groove density, the shear properties of the UHPC-NC grooved interface under compressive shear and pure shear stress states were analyzed by oblique shear test and double-sided shear test. Based on the test results, a formula for calculating the shear strength of the UHPC-NC grooved interface was proposed, along with the range of interface inclination angles for oblique shear specimens of such interfaces.The results show that the oblique shear specimen with an interface inclination angle of 30° exhibits NC compression damage or interfacial shear plus NC compression damage, while those with an interface inclination angle of 60° and direct shear specimens exhibit interfacial shear damage. The ultimate strength of specimens increases with the increase of NC strength. With the increase of groove density, the ultimate strength of inclined shear specimen with an interface angle of 30° remains basically unchanged, and the ultimate strength of inclined shear specimen with an interface angle of 60° and straight shear specimen gradually increases. The shear internal friction angle of the UHPC-NC grooved interface depends on the NC strength grade.

Key words: UHPC-NC grooved interface; interface shear strength; oblique shear test; double-sided shear test; groove density

收稿日期:2024-05-07;修订日期:2024-06-12

基金项目:"十四五"国家重点研发计划项目(2022YFC3002604);广东省省级科技计划项目(2021B1111610002);重庆市自然科学基金资助项目(CSTB2023NSCQ-MSX0811)

第一作者:田　静(1993—),女,河南焦作人,同济大学博士生.E-mail:1911677@tongji.edu.cn

通讯作者:杨新安(1964—),男,山西运城人,同济大学教授,博士生导师,博士.E-mail:xyang@tongji.edu.cn

现有隧道加固方法存在侵限、施工周期长和干扰屏蔽信号等缺点.因此,研发厚度小、施工周期短且抗干扰的隧道加固结构[1-2]具有重大意义.

超高性能混凝土(UHPC)具有超高的强度、韧性和耐久性[3-7].预制结构具有节省时间、对环境影响小等优点[8-10].将预制UHPC与后浇普通混凝土(NC)复合结构用于隧道加固,既能避免现有加固方法的弊端[11-13],还能减少UHPC的使用量,降低成本[14].良好的超高性能混凝土-普通混凝土(UHPC-NC)界面抗剪性能是发挥UHPC-NC复合结构承载性能的关键[15].结构界面一般使用专用模具形成规则刻槽以增强其抗剪性能.程文强等[16-21]通过直剪试验研究了刻槽和NC强度等级对UHPC-NC界面抗剪性能的影响.王鹏刚等[20]拟合得到了UHPC-NC界面的抗剪黏聚力计算公式.Tian等[1]通过直剪试验和斜剪试验研究了UHPC-NC刻槽界面在压剪复合应力状态下的剪切性能,但由于界面倾角选择不当,斜剪试件无法呈现界面破坏.目前,对UHPC-NC刻槽界面在纯剪应力状态下剪切性能的研究较多,但对其在压剪应力状态下的剪切性能以及界面抗剪强度计算方法的研究很少,斜剪试件的界面倾角选择不当是原因之一.

为此,本文考虑NC强度等级和刻槽密度2个因素,通过斜剪试验和双面直剪试验,分析了UHPC-NC刻槽界面在压剪和纯剪应力状态下的剪切性能,并基于试验结果提出UHPC-NC刻槽界面抗剪强度计算公式,求解斜剪临界倾角,为UHPC-NC刻槽界面的试验研究与设计应用提供参考.

1 试验

1.1 原材料

NC设计3个强度等级,分别为C30、C40和C50.UHPC中高强度钢纤维的体积分数为2%,长度为13.0 mm,直径为0.2 mm.UHPC由粉、石英砂、高强度钢纤维、减水剂和水组成,其用量分别为1 145.0、1 029.0、156.5、36.2、130.4 kg/m^3.根据GB/T 50081—2019《混凝土物理力学性能试验方法标准》和T/CBMF 37—2018《超高性能混凝土基本性能与试验方法》,测试了NC和UHPC的立方体抗压强度f_{cu}.UHPC的f_{cu}为135.0 MPa,NC的配合比和抗压强度见表1.

表1 NC的配合比和抗压强度

Table 1 Mix proportions and compressive strength of NC

Strength grade	Mix proportion/(kg·m^{-3})					f_{cu}/MPa
	Cement	Sand	Gravel	Admixture	Water	
C30	376.00	704.00	1 148.00	1.20	184.00	29.7
C40	415.00	552.00	1 288.00	4.15	165.00	56.1
C50	480.00	638.00	1 185.00	5.76	144.00	65.6

1.2 试件的设计与制作

1.2.1 试件的设计

刻槽密度ρ的计算式为:

$$\rho=\frac{nwk}{lk}=\frac{nw}{l} \tag{1}$$

式中:n为界面刻槽数量;k为界面宽度,mm;l为界面长度,mm;w为沿界面长度方向刻槽的宽度,mm.

设计3种刻槽表面,记为Gro Ⅱ、Gro Ⅲ、Gro Ⅳ,其对应的界面刻槽密度由式(1)计算,分别为0.133、0.266和0.399.斜剪试件的界面倾角α设为30°、60°.试件尺寸见图1,试验设计方案见表2.

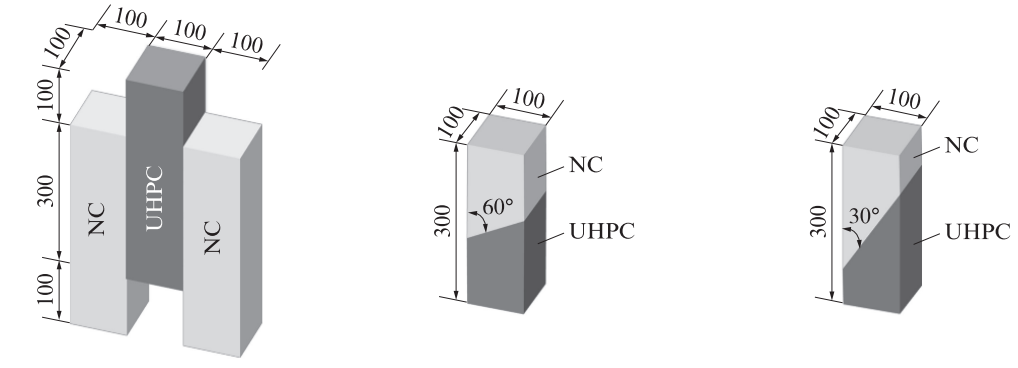

(a) Double-sided shear specimen (b) Oblique shear specimen, α=30° (c) Oblique shear specimen, α=60°

图1 试件尺寸

Fig. 1 Size of specimens(size: mm)

表2　试验设计方案

Table 2　Design schemes of test

Test	Strength grade	α/(°)	Grooved interface	Groove depth/width/number
Oblique shear test	C30/C40/C50	30	Gro Ⅱ	10 mm/15 mm/1
			Gro Ⅲ	10 mm/15 mm/2
			Gro Ⅳ	10 mm/15 mm/3
		60	Gro Ⅱ	10 mm/26 mm/1
			Gro Ⅲ	10 mm/26 mm/2
			Gro Ⅳ	10 mm/26 mm/3
Double-sided shear test	C30/C40/C50		Gro Ⅱ	10 mm/20 mm/2
			Gro Ⅲ	10 mm/20 mm/4
			Gro Ⅳ	10 mm/20 mm/6

1.2.2　试件制作

试件刻槽界面和模具见图2.采用木制模具制作,制作流程为:(1)将拌和好的UHPC倒入模具的对应区域,在振动台上振捣后,在15～25 ℃环境下养护3 d;(2)拆除界面处的木制模板;(3)将拌和好的NC倒入模具的相应区域,置于振动台上振捣,在15～25 ℃环境下养护3 d后脱模,自然养护至28 d.

1.3　加载与测试方案

分别采用3 000、1 000 kN的材料微机控制电液伺服万能试验机对斜剪试件和双面直剪试件进行加载.正式加载前对每1个试件进行预加载,预加载荷载为3 kN;正式加载时,斜剪试验加载速率为0.5 MPa/s,双面直剪试验加载速率为0.08 kN/s[1].采用非接触式数字散斑三维应变测量分析系统(XTDIC)记录直剪试件的变形和界面剪切应变,采样频率为4 s/张.

斜剪试件的极限强度σ_j(MPa)计算式为:

$$\sigma_j=\frac{F}{A} \tag{2}$$

式中:F为施加在试件上的极限荷载,N;A为试件的横截面面积,mm^2.

2　结果与分析

2.1　斜剪试验分析

2.1.1　破坏模式

斜剪试件的破坏模式见图3.由图3可见:(1)当α=30°时,C30斜剪试件的破坏模式均为NC压溃破坏;C40和C50的Gro Ⅱ界面斜剪试件破坏模式为界面剪切+NC压溃组合破坏;Gro Ⅲ和Gro Ⅳ界面斜剪试件的破坏模式为NC压溃破坏.(2)当α=60°时,所有斜剪试件的破坏模式均为界面剪切破坏.

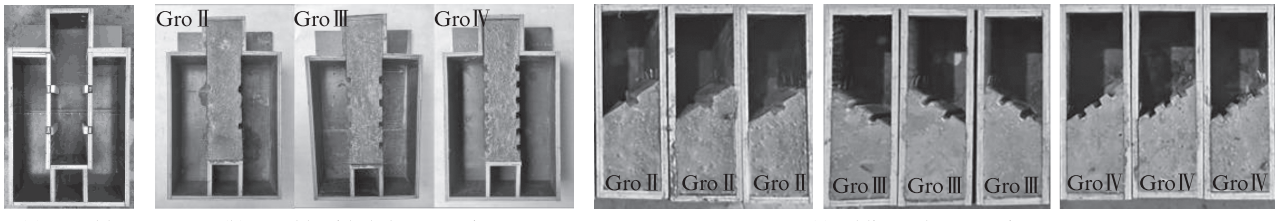

(a) Moulds　(b) Double-sided shear specimens　(c) Oblique shear specimens

图2　试件刻槽界面和模具

Fig. 2　Grooved interface and mold specimens

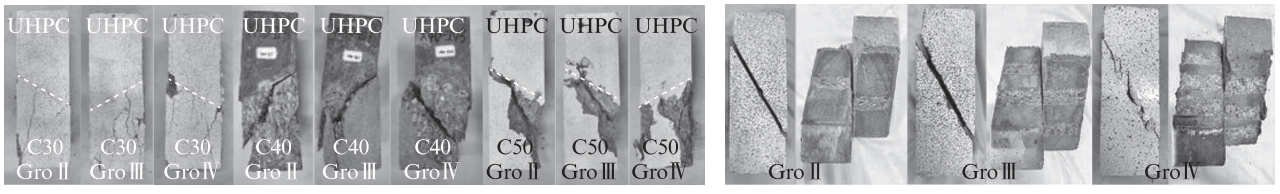

(a) α=30°　(b) α=60°

图3　斜剪试件的破坏模式

Fig. 3　Damage modes of oblique shear specimens

2.1.2　极限强度

刻槽密度对斜剪试件极限强度的影响见图4.由图4可见:(1)当α=30°时,随着刻槽密度的增大,斜剪试件的极限强度基本不变,且与NC抗压强度基本相等.(2)当α=60°时,斜剪试件的极限强度与刻槽密度呈正相关,但均小于NC的抗压强度.这是因为破坏模式为界面剪切+NC压溃组合破坏或NC压溃破坏的斜剪试件,其极限强度均取决于NC的抗压强度;破坏模式为界面剪切破坏的斜剪试件,其极限强度取决于界面的抗剪强度.界面刻槽密度越大,斜剪试件的极限强度越高;NC强度等级越高,斜剪试件的极限强度越大.(3)α=30°斜剪试件的极限强度均大于α=60°的斜剪试件.

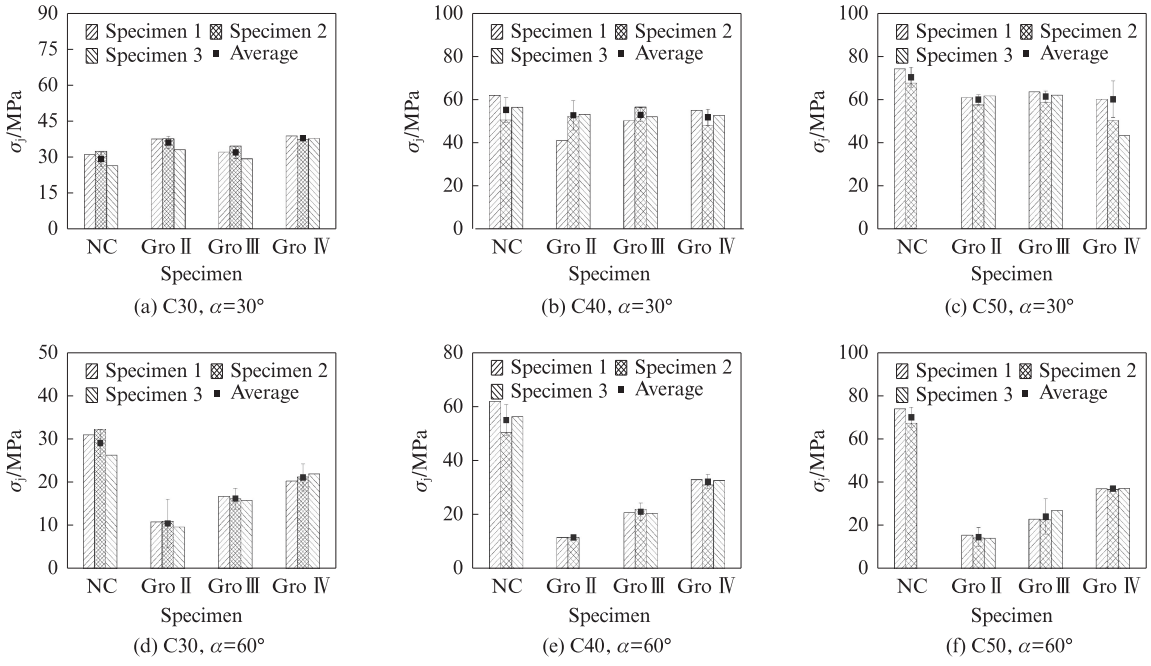

图4 刻槽密度对斜剪试件极限强度的影响

Fig. 4 Effect of groove density on ultimate strength of oblique shear specimens

2.2 双面直剪试验分析

2.2.1 破坏模式

双面直剪试件的界面剪应变分布见图5.由图5可见:对于发生双面剪切破坏的试件,两界面在破坏前后均产生较大的应变,两界面共同承载,双面直剪试件受力均匀;对于单面剪切破坏的试件,根据破坏时未发生破坏的界面是否产生明显应变,破坏形态可分为未破坏界面产生明显应变(见图5(b))和未破坏界面无明显应变(见图5(c))两种,均说明双面直剪试件两界面受力不均匀,破坏界面受力大,未破坏界面受力小.双面直剪试件非对称承载的原因可能是试件制作不标准.

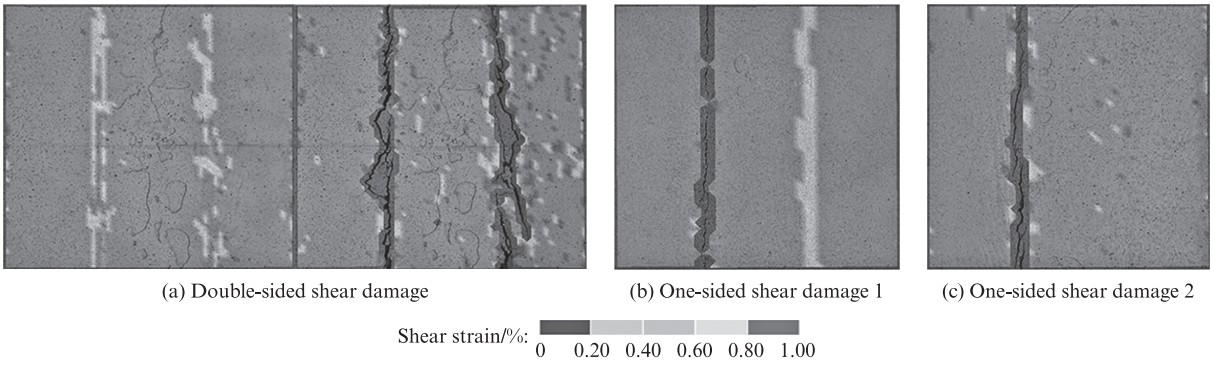

图5 双面直剪试件的界面剪应变分布

Fig. 5 Interface shear strain distribution of double-sided shear specimens

双面直剪试件的破坏模式见图6.由图6可见,双面直剪试件均呈现自然界面黏结破坏+键槽处NC被剪断的界面破坏模式,破坏形态有双面剪切破坏和单面剪切破坏两种.根据试件破坏时的形态和表面剪切应变分布情况,将双面直剪试验的界面破坏模式分为3种:(1)破坏模式A——双面剪切破坏;(2)破坏模式B——单面剪切破坏,且未破坏界面无明显应变;(3)破坏模式C——单面剪切破坏,但未破坏界面产生明显应变.由图6还可见,Gro Ⅱ界面双面直剪试件呈现破坏模式A、B和C,Gro Ⅲ和Ⅳ界面双面直剪试件呈现破坏模式A、B.所有试件双面直剪破坏模式见表3(C40,Gro Ⅱ界面双面直剪试件3因制作问题,无此项).

2.2.2 极限强度

同组试件中,破坏模式A的试件极限荷载约为破坏模式B试件的2倍.由于破坏模式B的试件未破坏界面无明显应变,可认为该类试件荷载完全由破坏界面承担.仅有1个试件破坏模式为C,且两界面

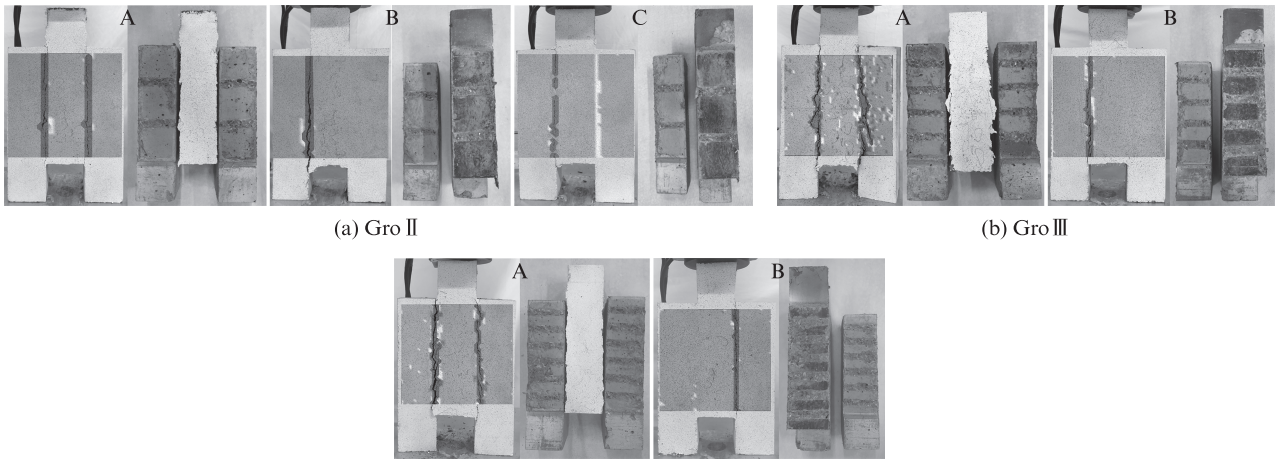

(a) Gro Ⅱ　　(b) Gro Ⅲ

(c) Gro Ⅳ

图6　双面直剪试件的破坏模式

Fig. 6　Damage modes of double-sided shear specimens

表3　所有试件双面直剪破坏模式

Table 3　Double-sided shear damage modes of all specimens

Strength grade	Grooved interface	Ultimate load (specimen 1/ specimen 2/ specimen 3)/kN	Failure mode (specimen 1/ specimen 2/ specimen 3)
C30	Gro Ⅱ	77.71/70.05/63.80	A/A/C
	Gro Ⅲ	55.38/103.20/57.08	B/A/B
	Gro Ⅳ	147.80/109.07/148.42	A/A/A
C40	Gro Ⅱ	52.54/58.30	B/B
	Gro Ⅲ	168.81/190.40/160.99	A/A/A
	Gro Ⅳ	210.93 /216.60/197.89	A/A/A
C50	Gro Ⅱ	73.90/70.00/73.80	B/B/B
	Gro Ⅲ	200.98/212.70/193.75	A/A/A
	Gro Ⅳ	120.80/247.60/242.56	B/A/A

承载比例无法确定,强度分析舍去该结果.

破坏模式A双面直剪试件的极限强度τ_A为:

$$\tau_A=\frac{F}{2A} \tag{3}$$

破坏模式B双面直剪试件的极限强度τ_A为:

$$\tau_A=\frac{F}{A} \tag{4}$$

刻槽密度对双面直剪试件极限强度的影响见图7.由图7可见:双面直剪试件的极限强度与刻槽密度呈正相关;NC强度等级越高,直剪试件极限强度越大.

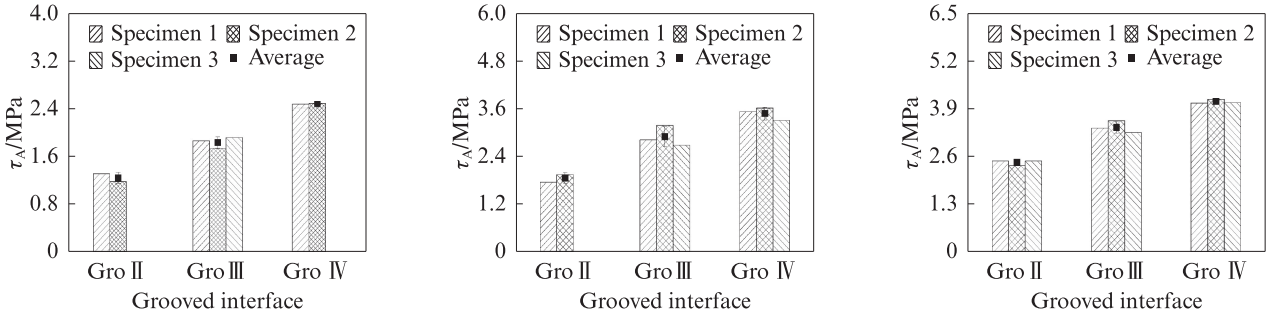

(a) C30　　(b) C40　　(c) C50

图7　刻槽密度对双面直剪试件极限强度的影响

Fig. 7　Effect of groove density on ultimate strength of double-sided shear specimens

2.3　UHPC-NC刻槽界面抗剪强度计算公式

界面倾角α的斜剪试件界面正应力σ和界面切应力τ分别为:

$$\sigma=\sigma_j\cos^2\alpha \tag{5}$$

$$\tau = \sigma_j \cos\alpha \sin\alpha \tag{6}$$

当界面切应力达到界面抗剪强度 τ_{int} 时，UHPC-NC刻槽界面试件表现为界面破坏.由摩尔-库伦定律可知，界面抗剪强度与界面正应力的关系为：

$$\tau_{int} = \sigma \tan\varphi + c \tag{7}$$

式中：φ 为界面的抗剪内摩擦角，(°)；c 为界面的抗剪黏聚力，MPa.

通过拟合双面直剪试件和 $\alpha=60°$ 斜剪试件破坏时的界面正应力和切应力，可以得到UHPC-NC刻槽界面的抗剪强度包络线，结果见图8.由图8可见，即使刻槽密度不同，相同NC强度等级试件刻槽界面的内摩擦角正切值基本相等；C30、C40、C50试件刻槽界面的内摩擦角正切值分别为1.27、1.25和1.18，可见刻槽界面的内摩擦角正切值随着NC强度等级的增大有减小的趋势.由此可见，UHPC-NC刻槽界面的抗剪内摩擦角取决于NC的强度等级，与刻槽密度基本无关.

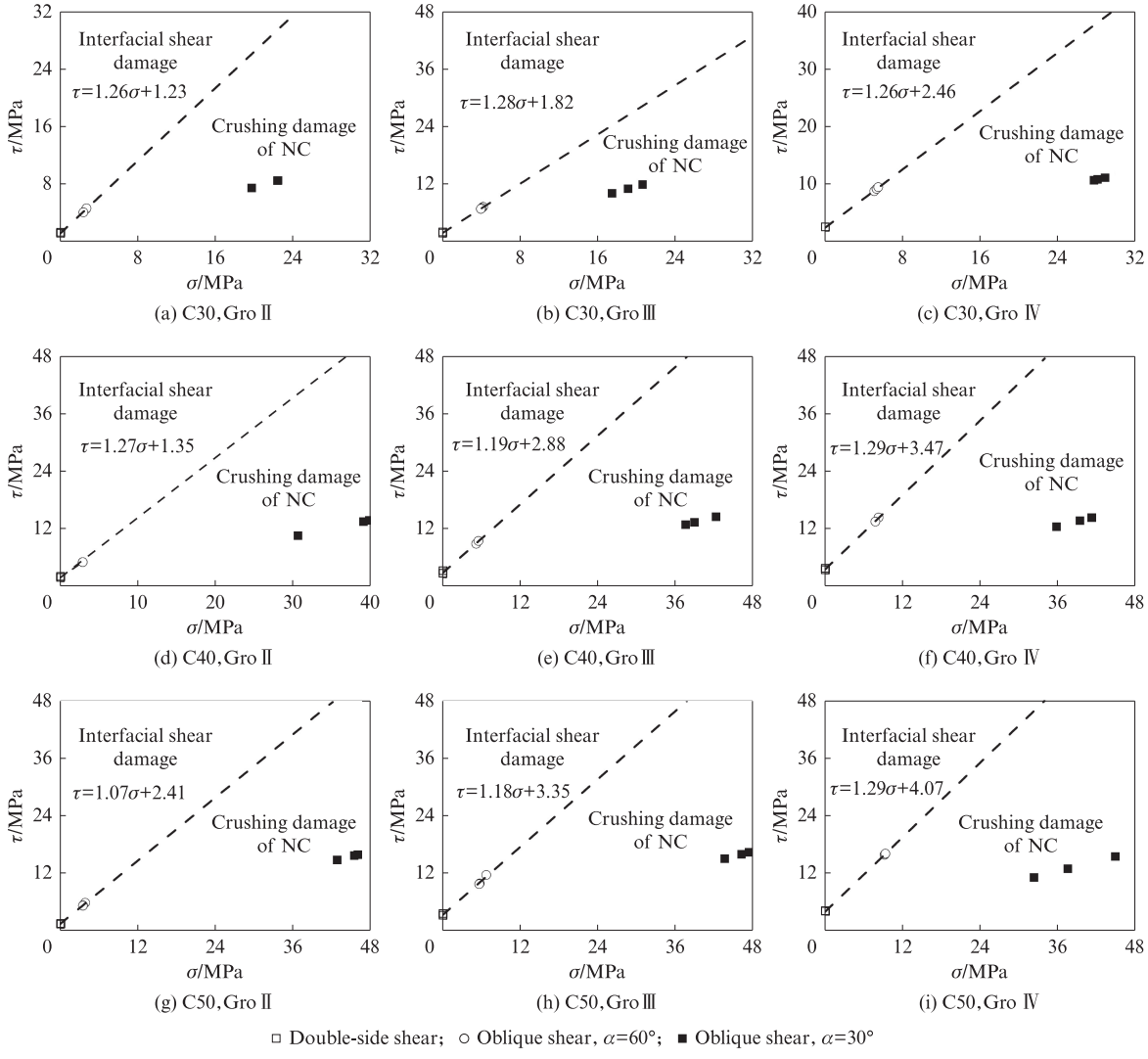

图8 UHPC-NC刻槽界面的抗剪强度包络线

Fig. 8 Shear strength envelopes of UHPC-NC grooved interface

在Tian等[1]的研究中，UHPC-NC刻槽界面的抗剪黏聚力 c 与界面刻槽密度 ρ 的关系为：

$$c = (1-\rho)(0.157\tau_{NC} - 0.516) + \tau_{NC}\rho^{a+1} \tag{8}$$

$$\tau_{NC} = 0.7\sqrt{f_c f_t} \tag{9}$$

式中：a 为NC的刻槽系数，C30、C40、C50的 a 分别为 -0.29、-0.34 和 -0.41；τ_{NC} 为NC的抗剪强度，MPa；f_c、f_t 分别为NC的单轴抗压强度、抗拉强度标准值，MPa.

将式(8)代入式(7)，可得UHPC-NC刻槽界面的抗剪强度计算式为：

$$\tau_{int} = \sigma\tan\varphi + (1-\rho)(0.157\tau_{NC} - 0.516) + \tau_{NC}\rho^{a+1} \tag{10}$$

UHPC-NC刻槽界面抗剪强度计算值与试验值的对比见表4.由表4可见，UHPC-NC刻槽界面抗剪

表4　UHPC-NC刻槽界面抗剪强度计算值与试验值的对比

Table 4　Comparison between calculated and tested values of shear strength of UHPC-NC grooved interface(α=60°)

Strength grade	Grooved interface	σ/MPa	τ_{int}/MPa		Error/%
			Tested value	Calculated value	
C30	Gro Ⅱ	2.63	4.55	4.56	0.23
	Gro Ⅲ	4.06	7.02	7.03	0.11
	Gro Ⅳ	5.28	9.14	9.13	0.08
C40	Gro Ⅱ	2.94	5.08	5.47	7.67
	Gro Ⅲ	5.38	9.31	9.33	0.21
	Gro Ⅳ	8.02	13.88	13.30	4.19
C50	Gro Ⅱ	3.69	6.38	6.76	5.91
	Gro Ⅲ	6.07	10.50	10.49	0.06
	Gro Ⅳ	9.26	16.01	14.99	6.36

强度计算值与试验值的误差均小于15%.这说明用式(10)计算UHPC-NC刻槽界面的抗剪强度是可靠的.

2.4　斜剪试件的界面倾角范围

当界面发生剪切破坏时，斜剪试件的界面正应力σ和切应力τ满足：

$$(\tan^2\varphi+1)\sigma^2+(2c\tan\varphi-\sigma_j)\sigma+c^2=0 \quad (11)$$

斜剪试验显示：当界面倾角较大时，斜剪试件发生界面剪切破坏；当界面倾角较小时，斜剪试件发生NC压溃破坏.因此，存在斜剪临界界面倾角α_1，使得斜剪试件同时出现界面剪切破坏和NC压溃破坏，此时$\sigma_j=f_{cu.}$.将其代入式(11)，可得斜剪试件破坏时的界面正应力σ_1为：

$$\sigma_1=\frac{-(2c\tan\varphi-f_{cu})+\sqrt{(2c\tan\varphi-f_{cu})^2-4(\tan^2\varphi+1)c^2}}{2(\tan^2\varphi+1)} \quad (12)$$

将NC的立方体抗压强度代入式(12)，可得UHPC-NC刻槽界面的斜剪临界界面倾角，结果见表5.由表5可见，UHPC-NC刻槽界面的斜剪临界倾角最大值为57°.故本文建议，UHPC-NC刻槽界面斜剪试件的界面倾角应不小于60°.

表5　UHPC-NC刻槽界面的斜剪临界界面倾角

Table 5　Critical interface inclination angle of oblique shear for UHPC-NC grooved interface

Unit:(°)

Strength grade	Grooved interface		
	Gro Ⅱ	Gro Ⅲ	Gro Ⅳ
C30	54	56	57
C40	53	54	55
C50	52	53	54

3　结论

(1)界面倾角α=30°的超高性能混凝土-普通混凝土(UHPC-NC)刻槽界面斜剪试件表现为NC压溃破坏或界面剪切+NC压溃组合破坏模式；α=60°的UHPC-NC刻槽界面斜剪试件以及双面直剪试件均表现为界面剪切破坏模式.当发生界面剪切破坏时，UHPC-NC刻槽界面上的NC键槽被剪断.

(2)NC强度等级越高，UHPC-NC刻槽界面剪切试件的极限强度越大.当α=30°时，随着刻槽密度的增大，斜剪试件的强度基本不变，且与NC的抗压强度基本相符；当α=60°时，刻槽密度越大，斜剪试件的强度越大，但始终小于NC的抗压强度.直剪试件的强度与刻槽密度呈正相关.

(3)UHPC-NC刻槽界面的抗剪内摩擦角取决于NC的强度等级.C30、C40、C50试件刻槽界面的内摩擦角正切值分别为1.27、1.25、1.18.

(4)提出了UHPC-NC刻槽界面的抗剪强度计算公式，并建议UHPC-NC刻槽界面斜剪试件的界面界面倾角应不小于60°.

参考文献：

[1] TIAN J, JIANG X H, YANG X N, et al. Bonding performance of the grooved interface between ultrahigh performance concrete and normal concrete[J]. Construction and Building Materials, 2022, 336:127525.

[2] WANG Y K, JIANG X H, LI K, et al. Experimental study of interfacial adhesion performance of prefabricated UHPC-NC diagonal shear groove[J]. Case Studies in Construction Materials, 2023, 19:e02343.

[3] 朋改非，牛旭婧，赵怡琳.异形钢纤维对超高性能混凝土增强增韧的影响[J].建筑材料学报，2016，19(6):1013-1018.
PENG Gaifei, NIU Xujing, ZHAO Yilin. Effects of deformed steel fiber on strengthening and toughening of ultra-high performance concrete[J]. Journal of Building Materials, 2016, 19(6):1013-1018. (in Chinese)

[4] 葛晓丽，褚洪岩.再生砂超高性能混凝土力学性能研究[J].建筑材料学报，2020，23(4):810-815.
GE Xiaoli, CHU Hongyan. Mechanical properties of ultra-high performance concrete with recycled sand[J]. Journal of Building Materials, 2020, 23(4):810-815. (in Chinese)

[5] 张高展，王宇譞，葛竞成，等.轻集料对超高性能混凝土工作和力学性能的影响[J].建筑材料学报，2021，24(3):499-507.
ZHANG Gaozhan, WANG Yuxuan, GE Jingcheng, et al. Effect of lightweight aggregate on workability and mechanical properties

of ultra-high performance concrete [J]. Journal of Building Materials, 2021, 24(3):499-507. (in Chinese)

[6] ESMAEILI J, ROMOUZI V, KASAEI J, et al. An investigation of durability and the mechanical properties of ultra-high performance concrete (UHPC) modified with economical graphene oxide nano-sheets[J]. Journal of Building Engineering, 2023, 80:107908.

[7] 李力剑, 刘素梅, 徐凡丁, 等. 含粗骨料超高性能混凝土的单轴受拉力学性能[J]. 建筑材料学报, 2024, 27(2):167-173.
LI Lijian, LIU Sumei, XU Fanding, et al. Uniaxial tensile behavior of ultra-high performance concrete containing coarse aggregate[J]. Journal of Building Materials, 2024, 27(2): 167-173. (in Chinese)

[8] 郭江龙, 王亚威, 薛永涛, 等. 马蹄形预制初期支护结构数值计算与试验研究[J]. 建筑结构, 2023, 53(增刊1):2875-2882.
GUO Jianglong, WANG Yawei, XUE Yongtao, et al. Numerical calculation and experimental study of horseshoe-shaped prefabricated initial supporting structure[J]. Building Structure, 2023, 53(Suppl 1):2875-2882. (in Chinese)

[9] 郇昊霖, 李培楠, 刘俊, 等. 大直径盾构隧道内部装配式预制结构安装路径优化及应用[J]. 现代隧道技术, 2024, 61(1): 236-244.
HUAN Haolin, LI Peinan, LIU Jun, et al. Optimization and application of installation path of prefabricated structure in large-diameter shield tunnel[J]. Modern Tunnelling Technology, 2024, 61(1):236-244. (in Chinese)

[10] 郝鹏飞. 预制整体式弧形件施工质量控制指标研究[J]. 现代隧道技术, 2024, 61(1):245-251.
HAO Pengfei. Study on construction quality control criteria for prefabricated integrated arcuate members[J]. Modern Tunnelling Technology, 2024, 61(1):245-251. (in Chinese)

[11] CHEN R P, MA Q L, ZHANG Y, et al. Experimental study on the mechanical behaviour of eccentric compression short column strengthened by ultra-high-performance fibre-reinforced concrete [J]. Structures, 2021, 33:508-522.

[12] HUANG B T, ZHU J X, WENG K F, et al. Prefabricated UHPC-concrete-ECC underground utility tunnel reinforced by perforated steel plate:Experimental and numerical investigations [J]. Case Studies in Construction Materials, 2022, 16:e00856.

[13] CHEN R P, GAO B Y, RUAN S Q, et al. Experimental study on the mechanical behavior of segmental joints of shield tunnels strengthened by a steel plate-UHPC composite[J] Tunnelling and Underground Space Technology, 2024, 144:105536.

[14] 吴玥, 张阳, 刘颖峰, 等. 预制UHPC与后浇NC界面的抗剪性能[J]. 铁道建筑, 2023, 63(9):48-53.
WU Yue, ZHANG Yang, LIU Yingfeng, et al. Experimental and numerical analysis on interfacial shear resistance of prefabricated UHPC-post-cast NC interface[J]. Railway Engineering, 2023, 63(9):48-53. (in Chinese)

[15] HABER Z B, MUNOZ J F, DE LA VARGA I, et al. Bond characterization of UHPC overlays for concrete bridge decks: Laboratory and field testing [J]. Construction and Building Materials, 2018, 190:1056-1068.

[16] 程文强, 耿健, 柳根金, 等. 界面处理对预制UHPC与现浇NC界面抗剪性能的影响[J]. 建筑材料学报, 2024, 27(1):76-83.
CHENG Wenqiang, GENG Jian, LIU Genjin, et al. Effect of interfacial treatment on shear properties of precast UHPC and cast-in-place NC[J]. Journal of Building Materials, 2024, 27(1): 76-83. (in Chinese)

[17] 张阳, 吴洁, 邵旭东, 等. 超高性能混凝土-普通混凝土界面抗剪性能试验研究[J]. 土木工程学报, 2021, 54(7):81-89.
ZHANG Yang, WU Jie, SHAO Xudong, et al. Experiment on interfacial shear properties between ultra-high performance concrete and normal strength concrete[J]. China Civil Engineering Journal, 2021, 54(7):81-89. (in Chinese)

[18] 吴琛, 储福玮, 龚明子, 等. 免蒸养超高性能混凝土-既有混凝土界面粘结性能试验研究[J]. 材料导报, 2023, 37(24):163-170.
WU Chen, CHU Fuwei, GONG Mingzi, et al. Experimental investigation of interfacial bond behavior between non-autoclave curing ultra-high performance concrete and existing normal concrete[J]. Materials Reports, 2023, 37(24):163-170. (in Chinese)

[19] 王朋, 尤学辉, 史庆轩, 等. 带肋超高性能混凝土与普通混凝土结合面剪切性能[J/OL]. 土木与环境工程学报(中英文), 2024: 1-11[2024-04-21]. http://kns.cnki.net/kcms/detail/50.1218.TU.20231207.0856.002.html.
WANG Peng, YOU Xuehui, SHI Qingxuan, et al. Shear behavior of rib-treated interface between ultra-high performance concrete and normal concrete [J]. Journal of Civil and Environmental Engineering, 2024:1-11[2024-04-21]. http://kns.cnki.net/kcms/detail/50.1218.TU.20231207.0856.002.html.(in Chinese)

[20] 王鹏刚, 赵明海, 田砾, 等. 预制键槽式UHPC与后浇混凝土界面黏结抗剪性能[J]. 复合材料学报, 2024, 41(5):2633-2644.
WANG Penggang, ZHAO Minghai, TIAN Li, et al. Interface shear resistance of precast keyway UHPC and post-cast normal concrete [J]. Acta Materiae Compositae Sinica, 2024, 41(5): 2633-2644. (in Chinese)

[21] 王德弘, 沈彤, 鞠彦忠, 等. 后浇普通混凝土与预制UHPC的黏结受剪性能研究[J]. 建筑结构学报, 2020, 41(增刊2):411-419.
WANG Dehong, SHEN Tong, JU Yanzhong, et al. Study on shear bond behavior of post-cast normal concrete and precast UHPC [J]. Journal of Building Structures, 2020, 41(Suppl 2):411-419. (in Chinese)